Evidence of defect-induced ferromagnetism in $ZnFe_2O_4$ thin films.

C. E. Rodríguez Torres,[1] F. Golmar,[2] M. Ziese,[3] P. Esquinazi,[3] and S. P. Heluani[4]

[1]*IFLP-CONICET and Departamento de Física, Facultad de Ciencias Exactas, Universidad Nacional de La Plata, C.C. 67 (1900) La Plata, Argentina*

[2]*CIC nanoGUNE Consolider Nanodevices GroupTolosa Hiribidea 76, E-20018 Donostia, San Sebastian - Espaa*

[3]*Division of Superconductivity and Magnetism, University of Leipzig, D-04103 Leipzig, Germany*

[4]*Laboratorio de Física del Sólido, Dpto. de Física, FCEyT, Universidad Nacional de Tucumán, Tucumán, Argentina.*

Abstract

X-ray absorption near-edge and grazing incidence X-ray fluorescence spectroscopy are employed to investigate the electronic structure of $ZnFe_2O_4$ thin films. The spectroscopy techniques are used to determine the non-equilibrium cation site occupancy as a function of depth and oxygen pressure during deposition and its effects on the magnetic properties. It is found that low deposition pressures below 10^{-3} mbar cause iron superoccupation of tetrahedral sites without Zn^{2+} inversion, resulting in an ordered magnetic phase with high room temperature magnetic moment.

PACS numbers: 61.05.cj, 75.25.-j, 75.47.-m, 75.50.Bb

I. INTRODUCTION

Among the functional materials that are being intensely studied to fabricate novel spintronics devices, the spinel oxides appear as an important alternative to perovskites. Particularly, $ZnFe_2O_4$ can be a half-metallic, transparent conductor or ferrimagnetic insulator[1,2]. At low dimensions, changing the growth conditions the magnetic and electronic properties of the ferrites can be tuned to enhance the magnetic moment considerably and to produce conducting or insulating materials[3]. These properties are very important for the design and fabrication of multilayer structures to produce spin-polarized currents.

It is well known that bulk $ZnFe_2O_4$ crystallizes in the normal spinel lattice and that it is antiferromagnetic with a Néel temperature of about 10 K. Zn^{2+} occupies tetrahedral (A) and Fe^{3+} octahedral (B) sites. The interaction between magnetic Fe^{3+} moments is of superexchange type mediated by O^{2-} ions and results in the magnetic moments being antiparallel to each other. Since the superexchange interaction is stronger for the more closely situated cations and for the bond angle closer to 180^0, the superexchange interaction of A-O-B (J_{AB}) is the strongest, the B-O-B (J_{BB}) is weaker, and that of A-O-A (J_{AA}) is the weakest. Accordingly, the magnetic structure and properties of spinel-type oxides depend strongly on the relative strength of the various superexchange interactions. In a normal spinel, magnetic Fe^{3+} ions occupy only B-sites and the weak negative superexchange interaction among Fe^{3+} ions (J_{BB}) dominates the magnetic properties of $ZnFe_2O_4$ leading to a low Néel temperature and consequently, paramagnetic behavior at room temperature. The situation is different, however, when normal spinel ferrite becomes nanosized. Net magnetization at room temperature can be obtained for nanoparticles obtained by different methods such as, mechanical synthesis[4–6], solvothermal method[7], solgel[6], co-precipitation[3,8] and thin films deposited by sputtering[9] and by pulsed laser deposition[10]. Several works have suggested that, in this case, the ferrite displays a nonequilibrium cation distribution among the tetrahedral and octahedral sites altering its long-range magnetic ordering. As a consequence the magnetic response is drastically enhanced. It was reported that when the particle size decreases Fe^{3+} occupancy of both A and B sites in the nanocrystalline state changes and Zn ions are transferred from their equilibrium position sites A to B sites. However, there is still some lack of clarity concerning Zn non-equilibrium positions and their magnetic effects. It is thought that the occupation of B-sites by Zn^{2+} brings Fe^{3+} ions in

both A- and B-sites, and the strong superexchange interaction between Fe^{3+} ions in A- and B-sites forces Fe in B sites to align ferromagnetically causing high magnetization at room temperature[5,6,8,11,12]. In addition, several authors reported the clear dependence of magnetic response on the preparation process, apart from the particle size[13,14]. Furthermore, it was found that both, the magnetic properties and cation distribution are extremely dependent on deposition conditions[10,15].

Despite progress in the characterization, the spin configuration of nanosized ferrites is still unclear and under study[16]. As the spinel oxides are ferrimagnets involving two different sublattices, the resulting magnetic moment is strongly perturbed by defects in the structural lattice. In addition, there has been increasing evidence that magnetic order can be triggered by certain defects in materials that are nominally non magnetic like certain oxides[17–19] or pure graphite[20]. In a thin film deposition process many of these defects can be generated. Particularly, it was recently suggested that oxygen vacancies affect the magnetic properties of synthesized Zn-ferrite films grown at various oxygen pressures[21]. Also the oxygen vacancies could be responsible for the semiconducting behavior found in $ZnFe_2O_4$ thin films with high saturation magnetization at room temperature and high Curie temperature[10]. There is clearly some need of employing new experimental procedures using different techniques that can provide complementary information that may clarify several open issues in the subject[22].

X-ray absorption near-edge structure (XANES) technique together with simulations based on ab-initio XANES calculations such as code FEFF8.2 are powerful tools to identify the modification of Zn^{2+} and Fe^{3+} distribution from the equilibrium to the non-equilibrium state[5,9,23,24]. Additionally, Grazing Incidence X-ray Fluorescence (GIXRF) yield the composition, thickness and density of thin films[25,26].
XANES combined with GIXRF results in an interesting method to relate thickness-dependent electronic structure with magnetic properties[27]. XANES is not a surface technique by itself, since the attenuation length of hard X-rays is a few micrometres in any material. However, in the grazing-incidence geometry near the critical angle for total reflection, the X-ray beam is confined within a few nanometres of the surface. For film studies, this confinement has the considerable advantage of minimizing the substrate contribution.

In this work, the structural and magnetic properties of $ZnFe_2O_4$ films fabricated by pulsed laser deposition using different oxygen partial pressures are reported and discussed. XANES

spectroscopy combined with GIXRF was used to determine the non-equilibrium cation site occupancy as a function of depth and its effects on the magnetic properties. Our results show that the presence of defects as oxygen vacancies or iron situated on normally non-occupied A sites in the spinel structure could be the cause for the magnetism in the films.

II. EXPERIMENTAL

The $ZnFe_2O_4$ films were fabricated by pulsed laser deposition (PLD) from a stoichiometric target onto MgO (001) substrates. Substrate temperature was 500^0C and the oxygen partial pressure was varied between 10^{-5} and 10^{-1} mbar. After deposition the samples were cooled to room temperature in vacuum at a pressure of about 10^{-7} mbar.

X-ray diffraction measurements employing Cu K_α radiation in a Philips X-Pert were made for structural characterization difractometer. Scanning Electron Microscopy, Supra 55VP, with Energy Dispersive Spectroscopy (EDS) was employed to study the surface morphology and spectral analysis. Magnetization measurements were made in a Quantum Design model MPMS-7 SQUID magnetometer. Magnetic fields were applied parallel to the films.

Electrical resistance measurements were performed using a Keithley 2182A Nanovoltmeter and a Keithley 6221 current source. Electrical contacts were made with gold wires clenched with indium. We have measured the resistance with a two-probe techniques.

GIXRF measurements were carried out at the XRF Fluorescence beamline of the LNLS (Campinas, Brazil), using a monochromatic X-ray beam of 9.7 keV. The setup includes 150 μ m-vertical and 4 mm slits limiting the beam size on the sample mounted on a high precision goniometer. Angular scans around the critical angle of total (external) reflection were performed (between 0 and 2 degrees). The fluorescence emissions were collected using a 15 element Ge detector. After the angular scan, XANES Fe K edge (7112 eV) and Zn K edge (9659 eV) spectra in fluorescence mode were collected at different grazing angles using a Si (111) channel-cut monochromator. The incident beam intensity and the energy calibration were monitored using an ion-chamber and a Co (or Zn) metal standard. The reflected beam and the Co (or Zn) fluorescence emission were collected using a second ion-chamber and a 15 element Ge detector, respectively.

Room temperature EXAFS (Extended X-ray Absorption Fine Structure) spectra at the Zn K-edge were recorded in flourescence mode using a Si(111) monochromator at the XAS2

beamline of the LNLS (Laboratorio Nacional de Luz Sincrotron) in Campinas, Brazil. In order to estimate the X-ray penetration depth for each incidence angle, the attenuation length as a function of incidence angle was estimated using the X-ray database of Lawrence Berkeley National Laboratory[28].

III. RESULTS AND DISCUSSION

X-ray diffractometry indicated epitaxial growth without any traces of secondary phases. φ-scans of the $ZnFe_2O_4$ (511) refection showed a fourfold symmetry of the film. Figure 1 shows the magnetic moment of the films as a function of applied field at room temperature (a) and at 5 K (b). The diamagnetic signal from the substrate was subtracted. The S-shaped M-H curves are evidence for ferrimagnetic order. In addition, a linear high-field response in room temperature measurements indicated the presence of a paramagnetic component. This was also deduced from M *vs.* T measurements (not shown here). The magnetic response diminishes by increasing the oxygen partial pressure from 10^{-5} to 10^{-1} mbar as seen by the decreasing of the magnetic moment by more than one order of magnitude. While at room temperature the coercivity is small, at low temperatures the films are magnetically rather hard with coercive fields between 447 mT and 1000 mT when deposition pressure varied from P = 10^{-5} to 10^{-1} mBar . The drastic reduction of coercive field at room temperature might indicate the existence of magnetic clusters and a blocking mechanism such as has been observed in references [6] and [9] for similar systems.

All films are insulating with room temperature resistivity larger than ρ= 100 Ωm. Sample ZF02 grown under 10^{-4} O_2pressure, had the smallest electrical resistance and we could measure its behavior under applied magnetic fields between 0.2 and 0.7 T and under light irradiation between 2.8 and 3.5 eV. The sample did neither present magnetoresistance nor photoconductivity in the range of fields and energies applied. SEM micrographs show uniform surfaces in all samples. These results suggest that the sample has a spatial uniform magnetic phase at room temperature and that the energy gap in this sample is larger than 3.5 eV.

In table I we summarized the results on characterization of samples labeled as ZFO1 to ZFO5.

TABLE I: Measurement parameters of ZFO: Oxygen partial pressure p, film thickness t, Fe/Zn ratio, magnetic saturation moment measured at room temperature and 5 K.

sample	p (mbar)	t (nm)	Fe/Zn	M(RT)10^{-4} (emu)	M(5 K)10^{-4} (emu)
ZFO1	10^{-5}	57	1.8	1.4	5.0
ZFO2	10^{-4}	51	2.3	0.2	2.5
ZFO3	10^{-3}	43	1.9	0.1	1.9
ZFO4	10^{-2}	36	–	–	1.5
ZFO5	10^{-1}	17	1.8	–	0.3

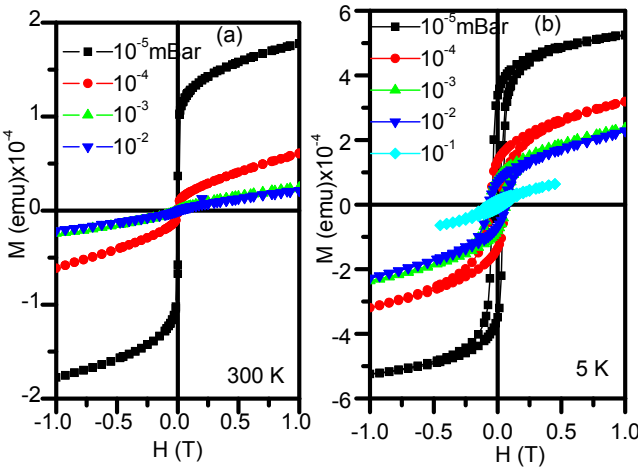

FIG. 1: Magnetic moment as a function of applied field at room temperature (a) and at 5 K (b) for the films prepared at different partial pressures.

Using the thicknesses in table I and the magnetic measurements, the estimated magnetization for sample ZFO1 are 100 emu/cm^3 and 360 emu/cm^3 at room temperature and 5 K respectively. These are large values considering that $ZnFe_2O_4$ with normal spinel structure is an antiferromagnet.

Figure 2 shows the intensity of Fe and Zn K_α lines as a function of incident angle for all films. The intensities are in arbitrary units and there is not direct relationship between intensities and concentration. The angle where a jump in intensity was observed (approximately 0.32 degree) corresponds to the total reflection condition. It can be observed that Zn/Fe fraction

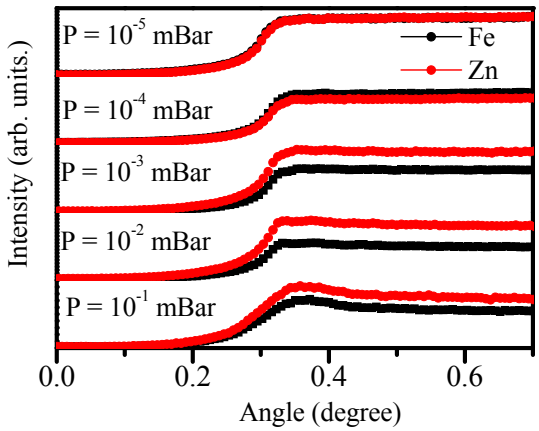

FIG. 2: Intensity of Fe and Zn K_α lines as a function of incident angle for all films. The intensities are in arbitrary units.

remains constant for all angles indicating a uniform distribution of both cations in depth. Furthermore, a Zn enrichment with the increase of oxygen pressure can be seen: the curve corresponding to Zn almost coincides with the Fe one for 10^{-5}mbar and this is above the Fe one for P=10^{-1} mbar. The XRF results were confirmed by EDS (see table I), although it can be seen that the ratio Fe to Zn is close to 2:1 independent of the O_2 growth conditions.

Figure 3 exhibits Zn (right) and Fe (left) K-edge XANES spectra, corresponding to samples 1, 2 and 5 taken at an incidence angle above total reflection (0.38 degree). The attenuation length for this angle was estimated as 35 nm, and then these spectra contain information from the inner of the film. The spectrum of powder $ZnFe_2O_4$ normal spinel was included for comparison. Zn K-edge spectra of normal spinel have three resolved peaks, A, B and C (indicated in Fig. 1) at around 9664, 9668 and 9672 eV, respectively, a shoulder at around 9677 eV (peak D), plus additional structure at higher energies (peak E). Zn K-edge spectra of samples 1 and 2 have similar characteristics of normal spinel. This indicates that in these films, Zn ions are mostly on A sites. In the case of sample ZFO5 the increase of peak B indicates that there is an important fraction of Zn on B sites[5,15,23].

Concerning Fe K-edge, in the case of normal ferrite, the edge position is expected for Fe^{3+} oxidation state and the pre-edge structure is characteristic of Fe in a distorted octahedrically coordinated environment that arises from electronic 1s→3d quadrupole and 1s→3d/4p hybridized orbitals dipole transitions. In XANES spectra of samples 2 and 5, the edge positions are close to $ZnFe_2O_4$ one but the white line amplitude is smaller which could indicate the

presence of Fe^{3+} with a coordination lower than 6[5,15]. Also the pre-peak amplitude are higher than the corresponding to normal ferrite indicating an increase of the degree of orbital p-d mixing that could indicate that the central Fe atoms occupy a more non-centrosymmetric environment.

The decrease of white line and the increase of the pre-peak intensities are larger for samples ZFO1 and ZFO2. Also the shift of the edge to lower energies observed for ZFO1 indicates the presence of Fe^{2+}. This sample, which has the highest magnetic moment, has the lowest white line intensity, the highest pre-peak amplitude and the lowest energy edge. The increase of B peak on Zn K-edge spectrum of ZFO5 could be indicative of inversion in normal spinel, i.e. Zn^{2+} in B sites and Fe^{3+} in A sites. However, in Fe K-edge spectrum the changes, compared with normal spinel, are minor and this film has the lowest Curie temperature and magnetic moment. In case of ZFO2 and ZFO5, which are ferromagnetic at room temperature, according to the Zn K-edge spectrum Zn ions are only in tetragonal A sites then, there is not inversion, but the decrease of white line and the increase of pre-peak indicates a decrease of Fe oxygen coordination and probably an increase of Fe in tetrahedral site.

In order to study differences between bulk and surface, we present now a comparison between XANES taken with incidence angle below and above total reflection angle (0.23 degree, attenuation length around 4 nm and 0.38 degree, attenuation length around 35 nm respectively).

In case of ZFO1 (Figure 3), no major changes were observed in the Zn K-edge. The decrease of peak C could be related to the elimination of multiple scattering paths due to the high contribution of surface atoms. The same can be observed for ZFO2 (see Figure 4). In Fe K-edge, the changes that evidence an increase of Fe in A sites and/or vacancies in the B site octahedron are less pronounced at the surface. In the case of ZFO5 (Figure 4) the tendency is similar but the difference with normal spinel is smaller.

Regarding XANES results, we can conclude that in the films grown at low pressure Zn^{2+} ions are in A sites (coordination four), and Fe^{3+} are octahedrically (B site) and tetrahedrically coordinated (A site). Also, there is fraction Fe^{2+} probably in B sites such as in Fe_3O_4 structure. The increase of Fe^{3+} in A sites and Fe^{2+} is favored by the deposition at low oxygen pressure and then due probably to the oxygen vacancy formation. A probe of that

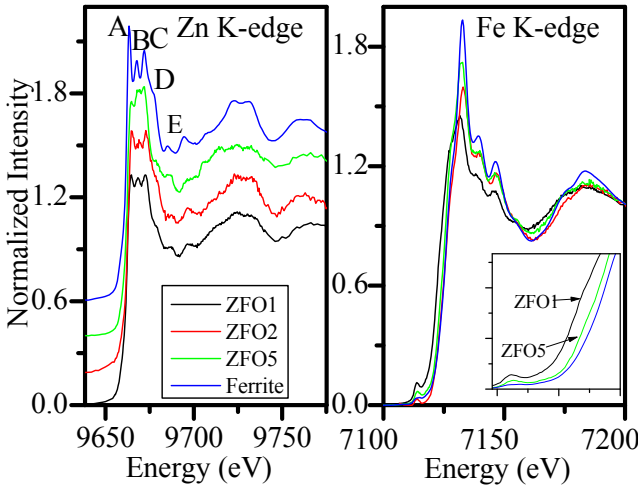

FIG. 3: (a) Zn and (b) Fe K-edge XANES using an incident of 0.38 degree, for films deposited at different oxygen pressures

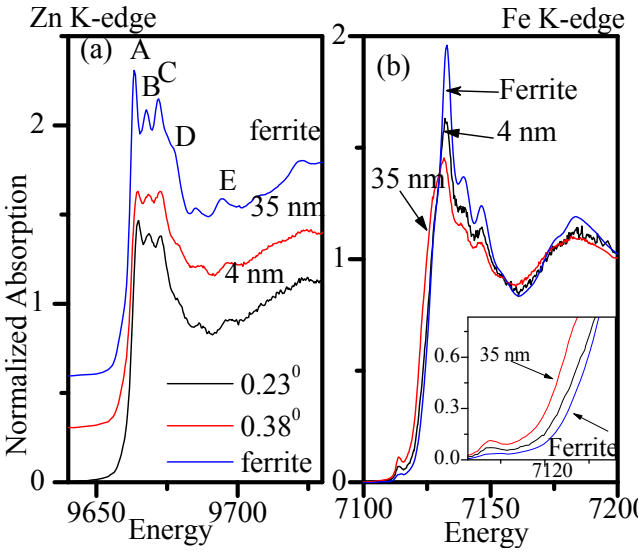

FIG. 4: (a) Zn and (b) Fe K-edges XANES, taken for film deposited at 10^{-4} mbar for two different incidence angles.

is the decrease of features in the XANES Fe K-edge taken with incidence angles lower than total reflection one, i.e. corresponding to the surface region where available environment oxygen neutralize oxygen vacancies. Then, in the case of low pressure growth films there is an increase of Fe^{3+} tetrahedral sites without inversion.

This significant result is supported by EXAFS. Figure 6 shows the Fourier transform

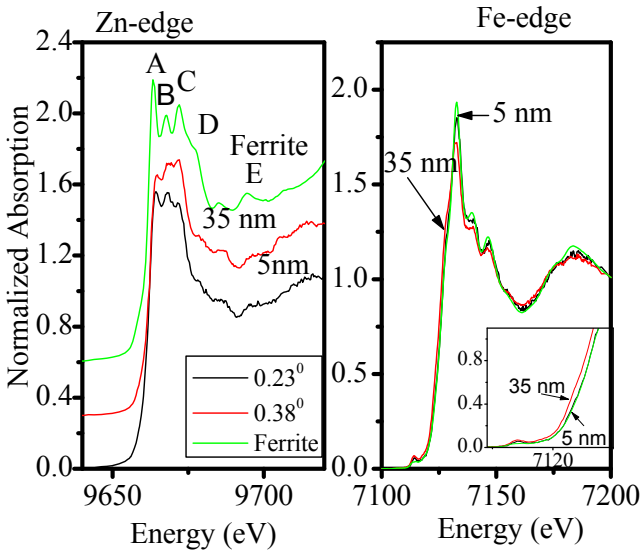

FIG. 5: (a) Zn and (b) Fe K-edge XANES, taken for film deposited at 10^{-1} mbar for two different incidence angles.

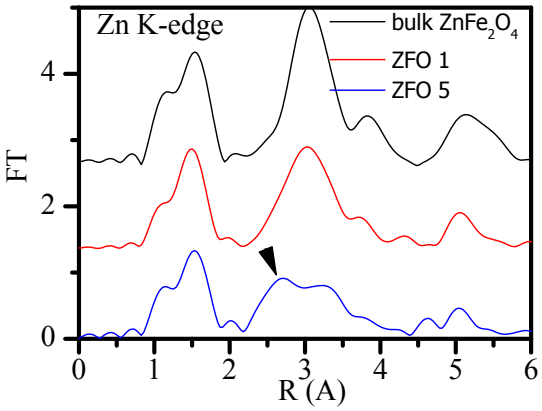

FIG. 6: Fourier transforms of $k^2\chi(k)$ oscillations (Zn K-edge) of bulk $ZnFe_2O_4$, ZFO1 and ZFO5 film ferrites . Arrow indicates the new coordination appear in FT of sample ZFO5 indicative that there are Zn atoms at B sites.

(FT) of oscillations extracted from Zn k-edge using Athena program of ZFO1 and ZFO5 films compared with FT of bulk $ZnFe_2O_4$ one.

FT of sample ZFO1 is qualitatively equal to bulk $ZnFe_2O_4$, reasserting that Zn atoms are in the tetrahedral sites. In the case of ZFO5, the presence of an additional peak around 2.6 A is an indicative that there are Zn atoms at octahedral sites[5].

The situation is different to the scenario found in references[5] and[9]: when Zn occupancy of 8-sites increases, Fe decreases, indicating some degree of inversion and magnetic response enhanced with such inversion. In our case the increase of Fe^{3+} in A sites is not due to Zn and Fe ions inversion, but the mechanism that explains the increase in the magnetization is probably the same as the one reported for inverse spinel. The increase of Fe^{3+} tetrahedrically coordinated (A site) increases Fe^{A}-Fe^{B} pairs antiferromagnetically coupled by superexchange, forcing Fe^{B}-Fe^{B} pairs to align ferromagnetically and also because Fe individual magnetic moments probably no longer cancel. The experimental results report in this work suggest that the increase of Fe^{3+} in A sites is not due to Zn and Fe ions inversion but of iron situated on normally non-occupied A sites in the spinel structure. In this structure only one eighth of the A sites in a unit cell are actually occupied and so some iron ions at these normally unoccupied sites will act as impurities and will not influence the crystallographic properties.

One more aspect in which oxygen pressure could influence is that as the magnetic interaction in the spinel is an indirect interaction, missing oxygen gives rise to a variation of exchange fields for the ions and a spin/glass like state is formed. Also, the reduction of Fe^{3+} ions into Fe^{2+} ions located in octahedral sites would strength ferromagnetic coupling between B-B sites such is the case in magnetite. In the case of Fe^{2+} located on the A sites there is an increase of magnetic moment due to the antiferromagnetic coupling with Fe^{3+} but the change will not be as big as for anti-sites.

In summary, we have shown that ferrites grown under low O_2 pressure conditions have a large magnetic moment. We found that the inversion mechanism is not responsible for the enhancements of the magnetic interaction – as was found in similar systems – but the presence of defects as oxygen vacancies or iron situated on normally non-occupied A sites in the spinel structure. We have also shown that controlling the oxygen pressure during the deposition, it is possible to obtain conductive or insulating Zn ferrites. These findings allow to control the magnetic and electric transport properties of spinel ferrites controlling the oxygen concentration.

Acknowledgments

We thank Dr. Silvana Stewart for fruitful discussions and Dr. Azucena Mudarra Navarro for collaboration in XAFS experiments.

This work was partially supported by Laboratorio Nacional de Luz Sincrotron, Campinas-Brasil; by CIUNT under Grants 26/E439 by ANPCyT-PICTR 20770 and 35682, by the German-Argentine PROALAR Grant Nr. D/08/11707 and the Collaborative Research Center SFB 762 "Functionality of Oxide Interfaces"

---

[1] A. Yanase and K. Siratori, J. Phys. Soc. Jpn. **53**, 312 (1984).

[2] U. Lders, A. Barthélémy, M. Bibes, K. Bouzehouane, S. Fusil, E. Jacquet, J. P. Contour, J.-F. Bobo, J. Fontcuberta, and A. Fert, Adv. Mater. **18**, 1733 (2006).

[3] S. Ayyappan, S. Philip Raja, C. Venkateswaran, J. Philip, and B. Raj, App. Phys. Lett. **96**, 143106 (2010).

[4] C. Yao, Q. Zeng, G. F. Goya, T. Torres, J. Liu, H. Wu, M. Ge, Y. Zeng, Y. Wang, and J. Z. Jiang, J. Phys. Chem. C **111** (2007).

[5] S. J. Stewart, S. J. A. Figueroa, J. M. Ramallo López, S. G. Marchetti, J. F. Bengoa, R. J. Prado, and F. G. Requejo, Phys. Rev. B. **75**, 073408 (2007.).

[6] J. H. Shim, S. Lee, J. H. Park, S. J. Han, Y. H. Jeong, and Y. W. Cho, Phys. Rev. B **73**, 064404 (2006).

[7] V. Blanco-Gutiérrez, F. Jiménez-Villacorta, P. Bonvilles, and R. Torralvo-Fernández, M. J. andSaez-Puche, J. Phys. Chem. C **115** (2011).

[8] T. Kamiyama, K. Haneda, T. Sato, S. Ikeda, and H. Asano, Solid State Com. **81**, 563 (1992).

[9] S. Nakashima, K. Fujita, K. Tanaka, K. Hirao, T. Yamamoto, and I. Tanaka, Phys. Rev. B **75**, 174443 (2007).

[10] Y. F. Chen, D. Spoddig, and M. Ziese, J. Phys. D: Applied Phys. **41**, 205004 (2008).

[11] F. K. Lotgering, J. Phys. Chem. Solids **27**, 139 (1966).

[12] S. Ligenza, Phys. Stat. Sol. **75**, 315 (1976).

[13] A. Kundu, C. Upadhyay, and H. Verma, Phys. Lett. A **311**, 410 (2003).

[14] S. D. Shenoya, P. A. Joyb, and M. R. Anantharaman, J. of Mag. and Mag. Mat. **269**, 217

(2004).

[15] J. Takaobushi, H. Tanaka, T. Kawai, S. Ueda, J.-J. Kim, M. Kobata, E. Ikenaga, M. Yabashi, K. Kobayashi, Y. Nishino, et al., Appl. Phys. Lett. **89**, 242507 (2006).

[16] K. Kamazawa, Y. Tsunoda, H. Kadowaki, and K. K., Phys. Rev. B. **68**, 024412 (2003).

[17] V. Fernandes, R. J. O. Mossanek, P. Schio, J. J. Klein, A. J. A. de Oliveira, W. A. Ortiz, N. Mattoso, J. Varalda, W. H. Schreiner, M. Abbate, et al., Phys. Rev. B. **80**, 035202 (2009).

[18] M. Khalid, M. Ziese, A. Setzer, P. Esquinazi, M. Lorenz, H. Hochmuth, M. Grundmann, D. Spemann, T. Butz, G. Brauer, et al., Phys. Rev. B. **80**, 035331 (2009).

[19] M. A. Ramos, J. Barzola-Quiquia, P. Esquinazi, A. Muoz-Martin, A. Climent-Font, and M. Garcí́a-Hernández, Phys. Rev. B. **81**, 214404 (2010).

[20] H. Ohldag, P. Esquinazi, E. Arenholz, D. Spemann, M. Rothermel, A. Setzer, and T. Butz, New Journal of Physics **12**, 123012 (2010), and refs. therein.

[21] M. Sultan and R. Singh, J. of Appl. Phys. **105**, 07A512 (2009).

[22] D. Darko Makovec, A. Alojz Kodre, I. Iztok Arcon, and M. Miha DrofenikDarko, J. Nanopart. Res. pp. DOI: 10.1007/s11051–010–9929–y (2010).

[23] S. J. A. Figueroa and S. J. Stewart, J. Synchrotron Rad. **16**, 63 (2009).

[24] M. Akhatar, M. Nadeem, S. Javaid, and M. Atif, J. of Phys. Cond. Matt. **21** (2009).

[25] J. Als-Nielsen, D. Jacquemain, K. Kjaer, F. Leveiller, M. Lahav, and L. Leiserowitz, Physics Report **246** (1994).

[26] K. Stoev and K. Sakurai, Spect. Acta Part B **54** (1999).

[27] N. Souza-Neto, A. Y. Ramos, H. Tolentino, and Y. Joly, J. of Phys.: Conf. Series. **190** (2009).

[28] B. Henke, E. Gullikson, and J. Davis, *X-ray interactions: photoabsorption, scattering, transmission, and reflection at E=50-30000 eV, Z=1-92*, vol. 54 of *2.* (Atomic Data and Nuclear Data Tables, 1993), 1st ed., 181-342.